Preparation of Porous Activated Carbon Materials and Their Application in Supercapacitors

Li Feng, Bing Yan, Changshui Wang, Qian Zhang, Shaohua Jiang, and Shuijian He

Abstract Porous carbon materials (PCMs) possess highly developed pore structure, and their pore size can range from molecular size to nano-size to large pores within micron size. As versatile materials with excellent physical and chemical properties such as large specific surface area, lightweight, high chemical stability, and electrical conductivity, PCMs have shown excellent application prospects in the fields of catalysis, adsorption, hydrogen storage, and energy storage. With the consumption of fossil energy and the rapid development of science and technology, the demands for high-performance supercapacitors are increasing day by day. PCMs are excellent electrode materials for supercapacitors. There are many methods to prepare PCMs, among which activation is the most widely used method. The activation methods can be divided into physical activation, chemical activation, and self-activation according to the activator used. In this chapter, the capacitance performance of PCMs synthesized via the activation process is summarized. The pore structure optimization process and the influence of pore structure on the capacitance performance of PCMs are also discussed. It is expected that this chapter could offer some enlightenments to the researchers' focus on improving the capacitance performance of PCMs.

Keywords Porous carbon · Carbonization · Activation · Supercapacitor

L. Feng · B. Yan · C. Wang · S. Jiang · S. He (✉)
Co-Innovation Center of Efficient Processing and Utilization of Forest Resources, International Innovation Center for Forest Chemicals and Materials, College of Materials Science and Engineering, Nanjing Forestry University, Nanjing, China
e-mail: shuijianhe@njfu.edu.cn

S. Jiang
e-mail: shaohua.jiang@njfu.edu.cn

Q. Zhang
College of Science, Nanjing Forestry University, Nanjing, China
e-mail: zhangqian5689@njfu.edu.cn

A. Uthaman et al. (eds.), *Advanced Functional Porous Materials*, Engineering Materials,
https://doi.org/10.1007/978-3-030-85397-6_19

1 Introduction

Porous carbon materials (PCMs) are important members in the big family of porous materials. PCMs could be prepared from various precursors including synthetic polymers, nature polymers, and carbon-rich small molecules (Borchardt et al. 2017; Gonzalez-Garcia 2018; Wang et al. 2020b). PCMs are widely applied in energy storage and conversion devices, electrocatalysis, water purification, electromagnetic shielding, microwave absorption, and other fields (Zhai et al. 2011; He et al. 2019c; Tian et al. 2020). PCMs show advantages in high yield, low cost, tunable microstructures, high specific surface area (SSA), stability, etc. Tons of PCMs are produced globally every year mainly from low cost biomass. The price of most PCMs could be below 1 $/g. The pore size of PCMs could be adjusted in the range of millimeter to micrometer to nanometer, and the corresponding specific surface area could be varied from a few square meters per gram to thousands square meters per gram. PCMs with pore size in the range of millimeter to sub-micrometer could be obtained from lyophilization/freeze drying, chemical blowing/(gas) foaming, template methods, etc. Usually, pores with the diameter below 100 nm are named nanopores. According to the classification of International Union of Pure and Applied Chemistry (IUPAC), nanopores can be divided into macropores (>50 nm), mesopores (2–50 nm), and micropores (0.2–2 nm). Micropores can be divided into super-micropores (>0.7 nm) and ultra-micropores (0.2–0.7 nm) (Liu et al. 2017). As to PCMs, ultra-micropores are always formed from the release of volatile gas and the condensation of carbon framework. The super-micropores of PCMs could be generated by the physical/chemical activation process (Yin et al. 2020). The formation of mesopores and macropores of PCMs always requires soft/hard templates within nano-size (Nishihara and Kyotani 2012; Zhu et al. 2019; Yan et al. 2021; He et al. 2019b).

Electrochemical double-layer capacitors (EDLCs) are relatively new energy storage devices which store the charge at the electrode/electrolyte interface, via physical ion adsorption/desorption process (He and Chen 2015; Simon et al. 2014). EDLCs possess the merits of high power density, good stability, easy maintenance, wide operating temperature, and low cost (Wang et al. 2016). PCMs are preferred electrode materials for EDLCs attributing to their good conductivity/stability, large specific surface area, tunable pore structure, and low cost (Merlet et al. 2012). The gravimetric specific capacitance of PCMs spans from a few Faraday per gram to hundred Faraday per gram mainly depending on the specific surface area and pore structure. In this chapter, the capacitance performance of PCMs synthesized via the physical/chemical activation process is summarized. The pore structure optimization process and the influence of pore structure on the capacitance performance of PCMs are also discussed. It is expected that this chapter could offer some enlightenments to the researchers' focus on improving the capacitance performance of PCMs.

2 Capacitance Performance of PCMs Synthesized with Activation Agents

PCMs are widely used as electrochemical energy storage devices because of their high SSA, multi-dimensional and tunable pore structure, good electrical conductivity, and low cost. Pore-size distribution and SSA are the main issues that dominate the performance of carbon-based supercapacitors. PCMs with large SSA and controllable pore size are good electrode materials for EDLCs. It is generally believed that microspores can enhance the electric double-layer capacitance of materials, mesopores provide low resistance channel for electrolyte ion transport, and macropores can be used as buffer reservoirs to store electrolyte ions (Wang et al. 2019). Activation is considered as an effective method to increase the SSA of carbon materials and introduce stratified porosity (Ding et al. 2021; He et al. 2013; Wang et al. 2020a).

Porous activated carbon is generally prepared from carbon precursors by the carbonization–activation approach. Activated carbon materials used in supercapacitors must meet the following three requirements: (1) a high SSA, (2) a low internal resistance, and (3) a microstructure conducive to the electrolyte entering the inner surface. High SSA is conducive to high specific capacitance. Low internal resistance determines high power density. Special pore structure is conducive to the formation of electrolyte wetting interface (Li et al. 2020c; Zhu and Xu 2020; Wang et al. 2020c).

The activation methods for preparing porous activated carbon can be divided into three categories: physical activation, chemical activation, and self-activation (Li et al. 2021b; Cao et al. 2021). In addition, it can be subdivided. Usually, the preparation process of porous activated carbon can be divided into one-step or two-step methods. One-step method means carbonization–activation occurs simultaneously. For the two-step method, the first step is carbonization, and the second step is activation that is using activator to further make pores. The different types of activation methods and its mechanisms, and some commonly used activators are described in detail below.

2.1 Physical Activation

Physical activation is usually carried out at high temperature (600–1200 °C) in the presence of oxidizing gases (Li et al. 2021b; Yin et al. 2020). Usually, air (Cai et al. 2020; Leng et al. 2017), carbon dioxide (Ding et al. 2021; Vinayagam et al. 2020; Elmouwahidi et al. 2020; Jin et al. 2016), and steam (Gao et al. 2020a; Qin 2019; Pallarés et al. 2018; Lee et al. 2016) can act as activation agents (Table 1). Most studies consider that activation temperature and activation time are the main factors affecting physical activation. Some studies have also investigated the effect of flow rate on pore structure (Qin 2019). Common physical activation methods are discussed in detail below.

Table 1 Summary of porous carbons produced by physical activation

Carbon source	Activating agent	SSA (m^2 g^{-1})	Mean pore size (nm)	Pore volume (cm^3 g^{-1})	Electrolyte	Specific capacitance	Energy density (Wh kg^{-1})	Power density (W kg^{-1})	Cycle life	References
Paper flower	$ZnCl_2$, CO_2	1801	3.28	1.16	1 M H_2SO_4	118 F g^{-1} (1 A g^{-1})	/	/	97.4% (10,000, 12 A g^{-1})	Veerakumar et al. (2020)
Bea pulp	CO_2	409	2.68	0.27	6 M KOH	106 F g^{-1} (0.25 A g^{-1})	1.7	2.11	93% (20,000, 10 A g^{-1})	Ding et al. (2021)
Spores	CO_2	3035	/	1.43	1 M $TEABF_4$/AN	305 F g^{-1} (1 A g^{-1})	56	60	93.85% (10,000, 2 A g^{-1})	Jin et al. (2016)
Formaldehyde and resorcinol	CO_2	1520	0.66	0.87	1 M H_2SO_4	235 F g^{-1} (0.125 A g^{-1})	5.94	54	100% (12,000, 1 A g^{-1})	Elmouwahidi et al. (2020)
Pine nut shell	Steam	956	2.59	0.62	6 M KOH	128 F g^{-1} (0.5 A g^{-1})	/	/	98% (10,000, 5 A g^{-1})	Qin (2019)
Polymer nanotubes	Steam	852	3.10	0.66	6 M KOH	276 F g^{-1} (1 A g^{-1})	/	/	98% (10,000, 1 A g^{-1})	Gao et al. (2020a)
Pitch-based CF	Steam	3230	/	1.89	1 M $(C_2H_5)_4NBF_4$/propylene carbonate	22.5 F g^{-1}	/	/	91.5% (20)	Lee et al. (2016)

(continued)

Table 1 (continued)

Carbon source	Activating agent	SSA (m^2 g^{-1})	Mean pore size (nm)	Pore volume (cm^3 g^{-1})	Electrolyte	Specific capacitance	Energy density (Wh kg^{-1})	Power density (W kg^{-1})	Cycle life	References
Activated hard carbon	Steam	2351	/	1.61	0.5 M Na_2SO_4	71 F g^{-1} (0.5 A g^{-1})	/	/	82.8% (5000, 5 A g^{-1})	Son and Park (2020)
Activated carbon	Steam	2156	1.87	1.01	2 M $TEABF_4/C_8H_{20}BF_4N$	187.2 F g^{-1} (0.5 A g^{-1})	/	/	92% (1000, 1 A g^{-1})	Li et al. (2017)
Dead pine needles	Air	783	2.55	0.49	1 M H_2SO_4	223 F g^{-1} (0.5 A g^{-1})	/	/	98% (10,000, 10 A g^{-1})	Leng et al. (2017)

2.1.1 Carbon Dioxide Activation

CO_2 is widely distributed on the earth and is rich in content. In those oxidizing gases, CO_2 can be used as an environment-friendly activator of materials, which is not only green but also easy to deal with, and has a good application prospect (Li et al. 2020c). The activation mechanism of CO_2 is shown in Eq. (1) (Navarro et al. 2007). In general, the CO_2 activation degree is mainly affected by the activation temperature, time, and the concentration of CO_2 (Zhu and Xu 2020).

$$C + CO_2 \rightarrow 2CO \tag{1}$$

Veerakumar et al. studied the capacitance performance of porous carbon nanosheets prepared by the carbonization of paper flower via chemical and physical activation (Veerakumar et al. 2020). The effect of CO_2 activation temperature on the SSA and pore-size distribution of the carbon materials was discussed. The influence on the capacitance performance of paper flower-derived carbon materials was also analyzed. They first activated the carbon material with $ZnCl_2$, followed by CO_2 activation at 700 °C and 800 °C, respectively (Fig. 1). The results show that the sample PFC-800 has the maximum SSA and pore volume, which are 1800 m^2 g^{-1} and 1.16 cm^3 g^{-1}, respectively. In a three-electrode system, the specific capacitances of PFC-800 are 91.2 F g^{-1} at 12 A g^{-1} which is more than twice the value of PFC-700 (44.9 F g^{-1}). The cycle stability of PFC800 is better than that of the activated sample at 700 °C, with a loss of only 3% after 10,000 charge–discharge cycles. They also studied the adsorption capacity of the carbon material to sunset yellow, as shown in the lower right corner of Fig. 1a, and found that PFC-800 had a good adsorption capacity to this pigment (273.6 mg g^{-1}). Elmouwahidi et al. prepared a kind of carbon microsphere and then activated it with CO_2 to investigate the effect of activation time (30, 60, 90, 120 min at 900 °C) on the material's pore structure (Elmouwahidi et al. 2020). Their results indicate that in the process of CO_2 activation, micropores are mainly produced, and the increase of micropores is especially obvious after 30 min, but the rise decreases when the time exceeds 60 min and reaches the peak at 90 min. After activation for 30 min, the formation of ultra-micropores is detected. With the time extension, the pores became wider. When the activation time increases to 90 min, the SSA (1523 m^2 g^{-1}), average pore size (0.95 nm), and pore volume all reach the maximum. Although CO_2 can play an active role in opening and expanding the pores, different activation conditions can produce different pore structures and SSA and influence the capacitance performance of porous carbon.

2.1.2 Steam Activation

As one of the commonly used physical activation methods, steam activation is not only cheap and easy to operate, but also an environmentally friendly activating agent. Steam activation is beneficial to the expansion of micropores, and thus, the activated carbon prepared by this activation method has a lower micropore volume (Zhu and

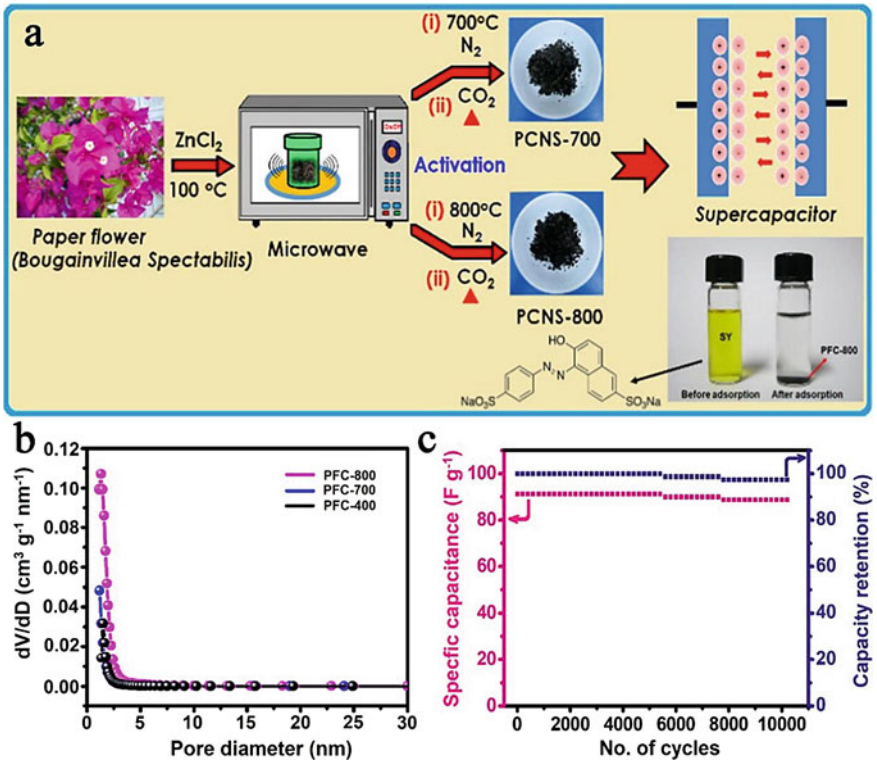

Fig. 1 **a** Preparation schematic of PFC, **b** the pore diameter of PFC samples at different activation temperatures, **c** cyclic performance of PFC-800 (Veerakumar et al. 2020)

Xu 2020; Pallarés et al. 2018). The steam activation mechanism is shown in Eq. (2). First, water vapor is adsorbed on the surface of the carbon, releasing hydrogen and oxygen (Navarro et al. 2007). Then, the presence of hydrogen prevents the continuous reaction of the active site, and the released oxygen further reacts with the carbon monoxide separated from the surface of the carbon to form carbon dioxide and at the same time produces a large number of micro-/mesopores (Sevilla et al. 2021; Li et al. 2020c; Yin et al. 2020).

$$C + H_2O \rightarrow CO + H_2 \tag{2}$$

For the stream activation process, the main factors affecting the pore structure of ACs are the activation temperature, activation time, and steam flow rate (Qin 2019). Lee et al. studied the capacitance performance of pitch-based activated carbon fibers (ACFs) produced by steam activation for different times (Lee et al. 2016). At the fixed activation temperature of 900 °C, the activation time was varied from 10 to 40 min. SSA of the as-prepared porous carbon spans from 1520 to 3230 $m^2\ g^{-1}$, and the pore volume increases from 0.61 $cm^3\ g^{-1}$ up to 1.87 $cm^3\ g^{-1}$. The specific capacitance

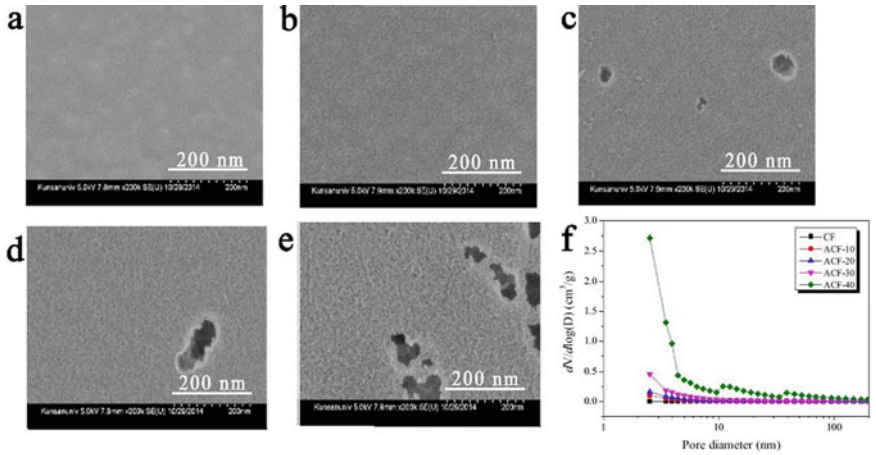

Fig. 2 **a**–**e** Scanning electron microscopy (SEM) images of activated carbon fiber with different steam activation times: **a** as-received CF, **b** ACF-10, **c** ACF-20, **d** ACF-30, **e** ACF-40, **f** the pore-size distribution curves of different samples (Lee et al. 2016)

increases from 1.1 to 22.5 F g^{-1}. Figure 2 shows that increasing activation time can produce larger pores, which also indicates that steam activation is conducive to mesopore development.

2.1.3 Air Activation

Compared with CO_2 and steam activation, air activation is less used and the activation temperature is lower. However, the redox reaction of oxygen and carbon is a severe exothermic reaction, and the direct use of air to activate carbon may cause excessive combustion of the raw materials and fail to effectively form pores (Li et al. 2020c). Leng et al. successfully synthesized activated carbon by carbonizing dead pine needles (PN) in the air at different temperatures (Leng et al. 2017). The products show pore volume of 0.25–0.49 cm^3 g^{-1} and SSA of 461–783 m^2 g^{-1}. In 1 M H_2SO_4 electrolyte, the PN-1000 exhibits a specific capacitance of 223 F g^{-1} at 0.5 A g^{-1} and maintains 150 F g^{-1} even at 100 A g^{-1}.

2.2 Chemical Activation

Chemical activation is one of the most used methods for the preparation of PCM (Table 2). Unlike physical activation, chemical activation takes place at slightly lower temperatures (i.e., 400–900 °C) and involves the dehydration by certain agents, such as phosphoric acid, zinc chloride, and alkaline hydroxide (Li et al. 2021b; Zeng

Table 2 Summary of porous carbons produced by chemical activation

Carbon source	Activating agent	SSA (m^2 g^{-1})	Mean pore size (nm)	Pore volume (cm^3 g^{-1})	Electrolyte	Specific capacitance	Energy density (Wh kg^{-1})	Power density (W kg^{-1})	Cycle life	References
Waste coffee grounds	H_3PO_4	763	/	0.47	1 M H_2SO_4	157 F g^{-1} (1 A g^{-1})	15	75	82% (10,000, 5 A g^{-1})	Huang et al. (2013)
Cotton stalk	H_3PO_4	1424	/	1.476	1 M H_2SO_4	341 F g^{-1} (0.5 A g^{-1})	/	/	94.3% (10,000, 1 A g^{-1})	Cheng et al. (2021)
Shiitake mushroom	H_3PO_4, KOH	2988	/	1.76	6 M KOH	306 F g^{-1} (1 A g^{-1})	8.2	100	95.7% (15,000, 3 A g^{-1})	Cheng et al. (2015)
Dry elm samara	KOH	1947	/	1.33	6 M KOH	470 F g^{-1} (1 A g^{-1})	25.4 (1 M EMIM BF_4)	15,000	98% (50,000, 10 A g^{-1})	Chen et al. (2016)
Soybean roots	KOH	2143	/	0.94	6 M KOH	276 F g^{-1} (0.5 A g^{-1})	100.5 (1 M EMIM BF_4)	4553	98% (10,000, 5 A g^{-1})	Guo et al. (2016)
Sorghum stem	KOH	1674	/	1.076	2 M KOH	257.2 F g^{-1} (1 mV s^{-1})	/	/	111% (12,000, 10 A g^{-1})	Kim et al. (2021)
Raw anthracite	KOH	3214	/	1.83	1 M $TEABF_4$-AN	172 F g^{-1} (0.5 A g^{-1})	37.2	303	93% (10,000, 1 A g^{-1})	Sun et al. (2020)
Butnea monsperma flower pollens	$ZnCl_2$	1422	2.16	0.77	6 M KOH	130 F g^{-1} (1 mA cm^2)	4.53	2070	99% (10,000)	Ahmed et al. (2019)

(continued)

Table 2 (continued)

Carbon source	Activating agent	SSA (m^2 g^{-1})	Mean pore size (nm)	Pore volume (cm^3 g^{-1})	Electrolyte	Specific capacitance	Energy density (Wh kg^{-1})	Power density (W kg^{-1})	Cycle life	References
Potato waste residue	$ZnCl_2$	1052	2.33	0.61	2 M KOH	255 F g^{-1} (0.5 A g^{-1})	/	/	93.7% (5000, 5 A g^{-1})	Ma et al. (2015)
Bean curd	CH_3COOK	2180	2.17	1.18	1 M H_2SO_4	430 F g^{-1} (0.1 A g^{-1})	12 (1 M H_2SO_4)	50	/	Li et al. (2018b)
Bean curd	CH_3COOK	1735	1.10	2.53	1 M H_2SO_4	315 F g^{-1} (0.1 A g^{-1})	8.5	50	93.5% (10,000, 1 A g^{-1})	Li et al. (2019)
Rape pollen	$CuCl_2$	2488	2.65	1.14	6 M KOH	390 F g^{-1} (0.5 A g^{-1})	26.8 (1 M Na_2SO_4)	181.4	92.9% (10,000, 20 A g^{-1})	Liu et al. (2018)
Rice husk	$CuCl_2$	1340	/	0.80	6 M KOH	152 F g^{-1} (20 A g^{-1})	/	/	100.1% (10,000)	Tian et al. (2019)
Enzymatic hydrolysis lignin	$CuCl_2$	1083	/	0.52	6 M KOH	736 F g^{-1} (1 A g^{-1})	49.3	500	100% (1000, 20 A g^{-1})	Chen et al. (2021)
Chitin	$CuCl_2$	1535	/	0.65	6 M KOH	227 F g^{-1} (0.5 A g^{-1})	5.2	/	94.3% (10,000, 10 A g^{-1})	Chen et al. (2019)
Cornstalk	NaCl KCl	1588	/	1.018	1 M H_2SO_4	407 F g^{-1} (0.5 A g^{-1})	14.35	123.9	96.2% (20,000, 5 A g^{-1})	Wang et al. (2018)
Java kapok tree shell	NaCl KCl	1260	1.24	0.439	6 M KOH	169 F g^{-1} (1 A g^{-1})	12.5	1900	97% (10,000, 1 A g^{-1})	Thileep Kumar et al. (2018)

(continued)

Table 2 (continued)

Carbon source	Activating agent	SSA (m^2 g^{-1})	Mean pore size (nm)	Pore volume (cm^3 g^{-1})	Electrolyte	Specific capacitance	Energy density (Wh kg^{-1})	Power density (W kg^{-1})	Cycle life	References
Cork	$KMnO_4$	1199	/	1.17	6 M KOH	290 F g^{-1} (0.2 A g^{-1})	14.7 (1 M Na_2SO_4)	395	95.2% (10,000, 5 A g^{-1})	Qiu et al. (2019a)
Foxtail grass seeds	$NaHCO_3$ $KHCO_3$	1428	2.30	0.821	6 M KOH	358 F g^{-1} (0.5 A g^{-1})	18.2 (1 M Na_2SO_4)	/	95.8% (10,000, 200 mV s^{-1})	Liang et al. (2021)
α-D-Glucose	$KHCO_3$	2230	/	1.05	1 M H_2SO_4	246 F g^{-1} (0.1 A g^{-1})	3.6	17,000	98% (5000, 5 A g^{-1})	Sevilla and Fuertes (2016)
Gelatin	$NaNO_3$	2872	/	1.618	1 M $EMIBF_4$	166 F g^{-1} (0.5 A g^{-1})	92	1000	92.2% (10,000, 5 A g^{-1})	Li et al. (2018a)
Soluble starch	$NaNO_3$	1864	/	2.22	6 M KOH	385 F g^{-1} (1 A g^{-1})	11.6	101	97.4% (8000, 2 A g^{-1})	Huo et al. (2020)
Albizia procera leaves	$NaHCO_3$ $ZnCl_2$	910	2.80	/	1 M H_2SO_4	231 F g^{-1} (1 A g^{-1})	32	625	97.3% (1000, 20 A g^{-1})	Mohamedkhair et al. (2020)
Chitosan	$FeCl_3$	807	/	0.93	1 M H_2SO_4	393 F g^{-1} (0.5 A g^{-1})	19.1	400	103% (8000)	Qiu et al. (2019c)
Mushroom	$FeCl_3$	1374	2.7	0.95	1 M H_2SO_4	307 F g^{-1} (1 A g^{-1})	6.6	1500	97.4% (8000, 2 A g^{-1})	Hou et al. (2018)

et al. 2014). Compared with physical activation, chemically activated porous carbon shows higher porosity development with porous network combining micropores and mesopores. Moreover, its selectivity is more extensive. At present, there are many kinds of chemical activators that have been used to prepare PCMs. The most used ones are KOH and $ZnCl_2$. Chemical activators can be divided into three main groups: acids, alkalis, and salts. The commonly used chemical activation methods are discussed below.

2.2.1 Acid Activation

Common acid activating agents include H_3PO_4 (Cheng et al. 2015, 2021; Budinova et al. 2006), H_2SO_4 (Kigozi et al. 2020), HNO_3 (Li et al. 2016; Pourhosseini et al. 2017; Zhu et al. 2017; Bo et al. 2018), etc. Phosphoric acid is used more often in those acidic activating agents. H_3PO_4 activation is related to its ability to promote bond cleavage and cross-linking formation. It can form phosphate bonds with the carbon precursors, resulting in a cross-linked structure. The activation process is roughly divided into six aspects as shown in Eqs. (3)–(8) (Myglovets et al. 2014; Olivares-Marín et al. 2006; Shi et al. 2019; Zhang et al. 2020):

$$n\mathrm{H_3PO_4} \xrightarrow{100\,^{\circ}\mathrm{C}\sim 400\,^{\circ}\mathrm{C}} \mathrm{H_{n+2}P_nO_{3n+1}} + (n-1)\mathrm{H_2O} \tag{3}$$

$$2\mathrm{H_3PO_4} \rightarrow \mathrm{P_2O_5} + 3\mathrm{H_2O} \tag{4}$$

$$2\mathrm{H_3PO_4} \xrightarrow{>500\,^{\circ}\mathrm{C}} \mathrm{H_2P_2O_7^{2-}} + \mathrm{H_2O} + 2\mathrm{H^+} \tag{5}$$

$$2\mathrm{H_2P_2O_7^{2-}} \rightarrow \mathrm{P_4} + 6\mathrm{O_2} + 2\mathrm{H_2O} \tag{6}$$

$$2\mathrm{P_2O_5} + 5\mathrm{C} \rightarrow \mathrm{P_4} + 5\mathrm{CO_2} \tag{7}$$

$$\mathrm{P_2O_5(liquid)} \rightarrow \mathrm{P_2O_5(gas)} \tag{8}$$

Cheng et al. first activated shiitake mushrooms with H_3PO_4 at 500 °C and then activated them with KOH for a second time (Cheng et al. 2015). The surface area of the activated sample (PAC-500) in the first step is 1341 $m^2\ g^{-1}$, and the pore volume is 2.02 $cm^3\ g^{-1}$. The size of pores formed is mainly between 2 and 5 nm, and considering that phosphoric acid reacts with carbon above 500 °C to form phosphate bond (Myglovets et al. 2014), so those nanopores are mainly due to the dehydration effect. After the activation of H_3PO_4, the rich channels are more conducive for the entry of KOH electrolyte into the interior, and the contact surface is larger to achieve a better effect. Finally, after two steps of activation and carbonization, the shiitake mushroom-derived carbon showed an interconnected hierarchical porous network.

The obtained hierarchical pores exhibited a high specific capacitance of 306 F g^{-1} at 1 A g^{-1} in KOH electrolyte; even when the current density rises to 30 A g^{-1}, the capacitance retention is 78.4%.

Unlike H_3PO_4, H_2SO_4 and HNO_3 activations mainly rely on their strong oxidizing property, not only can react with carbon atoms to produce some gas, which can achieve pore-forming, but also can enhance the surface wettability of the active porous carbon (Li et al. 2016; Zhu et al. 2017; Kigozi et al. 2020). Thus, enhance the capacitance performance of the carbon material.

2.2.2 Alkali Activation

Alkali activation is the most widely used activation method in chemical activation. The carbon materials are often activated by KOH to make pores to enhance the capacitive performance (Wang and Kaskel 2012). It was found that the KOH activation could inhibit the generation of tar, reduce the activation temperature, and accelerate the reaction rate. KOH activation also shows the advantages of high yield, low reaction temperature, high SSA, and micropore development (Kumar et al. 2020; Sun et al. 2020; Li et al. 2020c). Chemical activation mechanism of KOH is suggested as Eqs. (9)–(13) (Li et al. 2021b; Lozano-Castelló et al. 2007; Yin et al. 2020). KOH dehydration to form K_2O (Eq. 9) and then at about 400 °C is converted into K_2CO_3 (Eq. 10). At 600 °C, KOH is completely consumed. When the temperature rises to above 700 °C, K_2CO_3 and K_2O are reduced to metallic potassium (Eqs. 12–13). In the process of activation, CO_2, H_2O, CO, H_2, and other gaseous substances are released, which play the role of physical activation (Gao et al. 2020b; Sun et al. 2020; Wang et al. 2019; Li et al. 2020c; Yin et al. 2020).

$$2KOH \rightarrow K_2O + H_2O \tag{9}$$

$$K_2O + CO_2 \rightarrow K_2CO_3 \tag{10}$$

$$K_2CO_3 \rightarrow K_2O + CO_2 \tag{11}$$

$$K_2CO_3 + 2C \rightarrow 2K + 3CO \tag{12}$$

$$K_2O + C \rightarrow 2K + CO \tag{13}$$

The activation temperature (Guo et al. 2016; Kim et al. 2021; Sun et al. 2020; Li et al. 2020b), immersion time (Yakaboylu et al. 2021), concentration of KOH (Chen et al. 2016), and the mass ratio of carbon precursors to KOH (Guo et al. 2016; Lv et al. 2019; Mo et al. 2020; Yu et al. 2019) will affect the pore-size distribution, porosity, and SSA of the carbon materials. Guo et al. studied the influence of KOH/carbon source mass ratio and activation temperature on capacitive performance of soybean

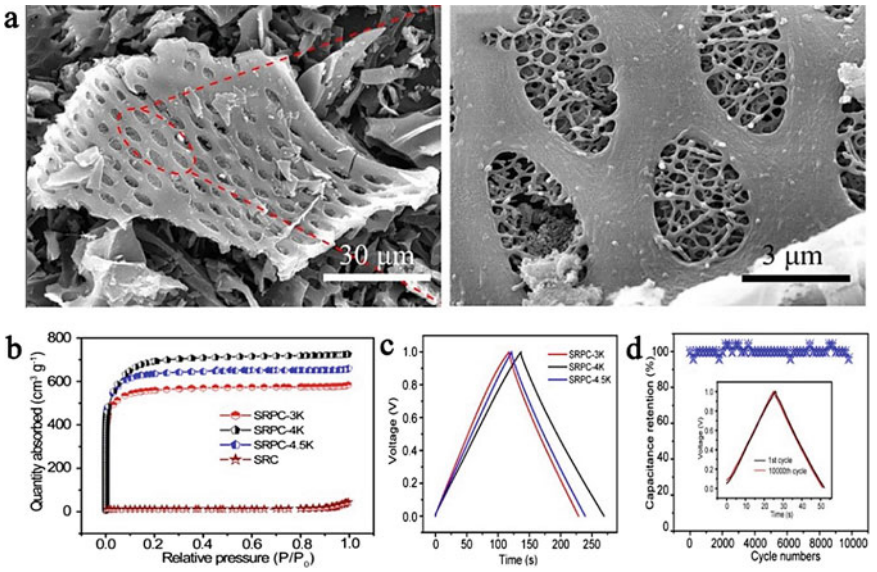

Fig. 3 **a** SEM images of SRPC-4K, **b** N_2 physisorption isotherms, **c** charge/discharge curves at 1 A g^{-1}, **d** cyclic stability at 5 A g^{-1} for 10,000 cycles of SRPC-4K (inset: charge/discharge curves of the 1st and 10,000th cycles) (Guo et al. 2016)

root-derived hierarchical porous carbon (SRPC) (Fig. 3) (Guo et al. 2016). When the mass ratio of KOH to soybean root is 4:1 and the activation temperature is 800 °C, the porous carbon obtained has the largest SSA (2143 m^2 g^{-1}) and the largest proportion of micropore SSA (1772 m^2 g^{-1}). The mesopore volume of SRPC-4K is 0.13 cm^3 g^{-1}, and the micropore volume is 0.81 cm^3 g^{-1}. It has the richest hierarchical micro-/mesoporous structure. The high microporosity is conducive to the accumulation of charge, and the mesopores can transport abundant electrolyte into the micropores, thus enhancing the capacitive performance of porous carbon. When used as electrodes of SC, SRPC-4K displays a high specific capacitance of 276 F g^{-1} at 0.5 A g^{-1} and 98% capacitance retention after 10,000 cycles at 5 A g^{-1} (Fig. 3d) in a two-electrode configuration in 6 M KOH electrolyte. In conclusion, although KOH activation is used for pore-forming, appropriate activation conditions are needed to achieve the best capacitance performance for different carbon sources.

2.2.3 Salt Activation

In addition to acid and alkali activation, there is a class of salt-activating agents. Those reagents include some metal chlorides, decomposable salts, and oxidizing salts.

Metal Chlorides

In the preparation of porous carbon, metal chlorides, such as $ZnCl_2$ (Ahmed et al. 2019; Li et al. 2021a; Ma et al. 2015), $FeCl_3$ (Bedia et al. 2018; Hou et al. 2018; Li et al. 2020a), NaCl (Wang et al. 2018; Zong et al. 2020; Thileep Kumar et al. 2018), KCl (Wang et al. 2018; Thileep Kumar et al. 2018), and $CuCl_2$ (Liu et al. 2018; Chen et al. 2019, 2021; Tian et al. 2019), are often used as activators.

$ZnCl_2$ is mainly acted as a dehydrating agent and can be deoxidized in the form of water (Zhu and Xu 2020). Beyond that, $ZnCl_2$ can also converted to ZnO (Eq. 14), which further etches carbon and be reduced to Zn (Eq. 15) (Kim et al. 2007; Wang et al. 2019). Better porous structure and higher carbon yield can be obtained. The activation temperature of $ZnCl_2$ is usually between 600 and 1000 °C. When the temperature is above 700 °C, $ZnCl_2$ volatilizes without post-treatment. The factors affecting the pore formation of $ZnCl_2$ are close to those of KOH, but the activation temperature and impregnation ratio are more important. Ahmed et al. used pollen as a carbon source, and they investigated the effect of impregnation ratio with zinc chloride on the pore structure of porous carbon (Ahmed et al. 2019). The optimum mesopore ratio can be obtained by the appropriate impregnation ratio. If the impregnation ratio is too large, $ZnCl_2$ will destroy the walls between adjacent micropores. It is confirmed that when the mass ratio of carbon source $ZnCl_2$ is 1:2, the SSA of the resulting porous carbon is 1422.66 $m^2\ g^{-1}$, the total pore volume is 0.77 $cm^3\ g^{-1}$, the micropore volume is 0.33 $cm^3\ g^{-1}$, and the mesopore volume is 0.44 $cm^3\ g^{-1}$. Using ionic liquid electrolyte, the activated carbons achieved large magnitudes of energy density (~42 Wh kg^{-1}) and power density (~19 kW kg^{-1}).

$$ZnCl_2 + 1/2O_2 \rightarrow ZnOCl + 1/2Cl_2 \tag{14}$$

$$2ZnO + C \rightarrow 2Zn + CO_2 \tag{15}$$

In recent years, some metal chlorides have also acted as molten salts, reacting with carbon at high temperatures to produce porous structures, which is so-called molten salt etching method. Wang et al. adopted non-toxic NaCl and KCl mixed salt as reaction media to regulate the activation process of corn straw (Wang et al. 2018). Hierarchical porous carbon sheets (HPCSs) with good capacitive properties were successfully prepared. They found that when the temperature is higher than 800 °C, Cl^- etched the carbon skeleton to form micro- and mesopores. The hierarchical porous carbon obtained by this strategy has a SSA of 1588 $m^2\ g^{-1}$ and a high specific capacitance of 407 F g^{-1} at 1 A g^{-1} in the three-electrode system.

$CuCl_2$ is another molten salt that can be used as an activation agent. The mechanisms of $CuCl_2$ porogen are described as Eqs. (16–17) (Liu et al. 2018)

$$3CuCl_2 + C + 2H_2O \rightarrow Cu + 2CuCl + CO_2 + 4HCl \tag{16}$$

$$4CuCl + C + 2H_2O \rightarrow 4Cu + CO_2 + 4HCl \tag{17}$$

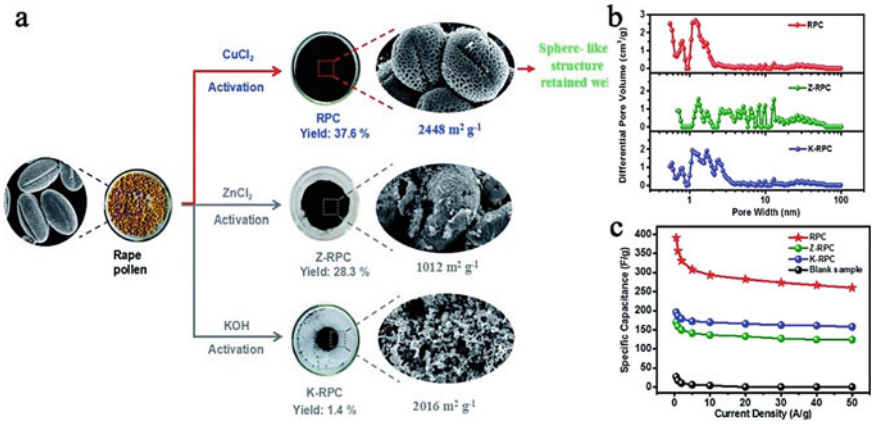

Fig. 4 **a** Schematic illustration of the preparation of RPC, **b** pore-size distribution (PSD) curves of RPC, Z-RPC, and K-RPC, **c** specific capacitances of RPC, Z-RPC, K-RPC, and the blank sample at different current densities (Liu et al. 2018)

The porous carbon can maintain the spherical shape (Fig. 4a) of the original carbon precursor, with the pores distributed below 2 nm and pore-size distribution centered at 1.2 nm. As is shown in Fig. 4b, under the same conditions, compared with the activation of $ZnCl_2$ (Z-RPC) and KOH (K-RPC), the pore-size distribution of the former is wide (1–60 nm), while that of the latter is mainly below 3 nm. Moreover, the porous carbon obtained by the activation of $CuCl_2$ shows a high SSA of 2488 $m^2\ g^{-1}$ and presents an outstanding gravimetric capacitance of 390 F g^{-1} at 0.5 A g^{-1} in 6 M KOH electrolyte (Fig. 4c). There is no doubt that molten salt etching is milder than acid/base activation, but it is more expensive and unsuitable for practical production.

Decomposable Salts

There are various salts that can be decomposed to produce gases, which can etch carbon to produce pores, such as carbonates (Mao et al. 2020; Ma et al. 2019; Tang et al. 2018), acetates (Li et al. 2018b, 2019), bicarbonates (Liang et al. 2021; Sevilla and Fuertes 2016), nitrates (Li et al. 2018a; Huo et al. 2020; Wang et al. 2017), and so on. Li et al. produced a macro- and mesoporous carbon material by using the decomposable and water-removable $NaNO_3$ as the porogen (Li et al. 2018a). Above 600 °C, $NaNO_3$ begins to decompose, generating N_2, O_2, and NO, which is conducive to the formation of mesopores (Eqs. 18 and 19) (Li et al. 2018a). The pore size of the material is affected by the dosage of $NaNO_3$. The modified carbon material showed small mesopores of 2–4 nm and larger mesopores of 5–50 nm, with a SSA of 2872.2 $m^2\ g^{-1}$. Due to the synergistic effect of suitable macro-mesoporous ion-diffusion channels and continuous conductive network, the porous carbon material exhibits a high power density. Huo et al. used $NaNO_3$ and KOH to activate soluble

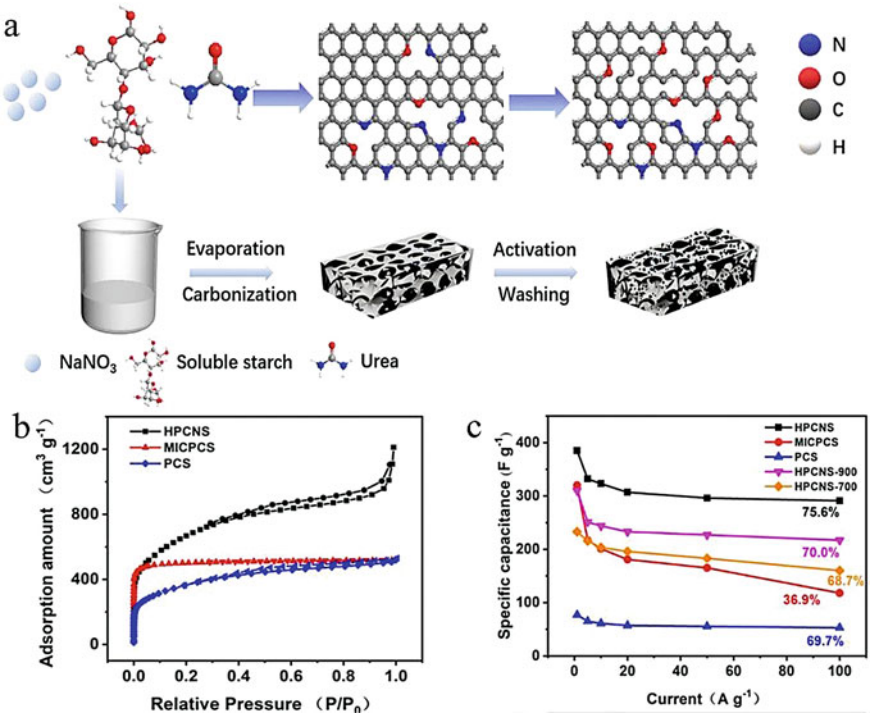

Fig. 5 **a** Schematic illustration of the synthesis of HPCNS, **b** N_2-adsorption/desorption isotherms, **c** specific capacitance as a function of the current densities (Huo et al. 2020)

starch to produce interconnected layered porous carbon networks (Fig. 5a) (Huo et al. 2020). As can be seen from Fig. 5b, the PCMs prepared by $NaNO_3$ and KOH activation (HPCNS) possess micropores, mesopores, and macropores at the same time. However, the materials prepared only with KOH (MICPCS) have no obvious mesoporous and macroporous characteristics. The results showed that the HPCN prepared at 800 °C had a maximum specific surface area of 1864 $m^2\ g^{-1}$ and a total pore volume of 2.22 $cm^3\ g^{-1}$. In a three-electrode system with 6 M KOH electrolyte, it shows good capacitance performance. The specific capacitance reaches 385 F g^{-1} at 1 A g^{-1}. Even when the current density is up to 100 A g^{-1}, HPCNs can achieve a capacitance retention of 75.6% (Fig. 5c).

$$12NaNO_3 \rightarrow 6Na_2O + N_2 + 10O_2 + 10NO \tag{18}$$

$$2Na_2O + C \rightarrow 4Na + CO_2 \tag{19}$$

Some oxidizing salts are also used in the preparation of porous activated carbon. For example, $KMnO_4$ gradually decomposes into oxygen, water-soluble potassium salt, and non-water-soluble manganese salt in the process of continuous pyrolysis,

which are beneficial to the formation of hierarchical pores (Qiu et al. 2019a, b; Yi et al. 2020). In addition, KNO_3 (Leng et al. 2020; Wang et al. 2017) can also be used as an oxidizing salt for the activation of porous carbon.

2.3 Self-activation

Although the above-mentioned activation methods and activation reagents have been widely used in the preparation of PCMs, they inevitably have some disadvantages, such as corrosive reagents, complex activation operation, post-treatment, and secondary pollution. Self-activation can simplify the activating process without the need for additional activation reagents and reducing the cost. Its pore generation mechanisms include three aspects: (1) chemical activation (it contains some inorganic salts, organic salts, and some special components, which can be used for activation), (2) physical activation (utilization of CO_2 and H_2O produced by pyrolysis), and (3) removal of inorganic nanoparticles in carbon source (Sevilla et al. 2021). The main influencing factors of self-activation are carbonization temperature and time (Wang et al. 2021; Gao et al. 2021; He et al. 2019a; Bhat et al. 2021). Niu et al. fabricated mesopore-dominant porous carbon as electrode materials by direct pyrolysis (600, 850, 900, 1000, 1100, 1200 °C) of cattle bones in an Ar atmosphere (Niu et al. 2017). With the increase of temperature, the surface of carbon changes from nonporous to porous. The porous carbon obtained at 1100 °C presented a hierarchical porous structure with a large SSA of 2096 $m^2\ g^{-1}$. The mesopore volume is 1.83 $cm^3\ g^{-1}$, and the conductivity reached 5141 S m^{-1}. PC-1100 displayed a high specific capacitance of 258 F g^{-1} at a current density of 5 A g^{-1} in a symmetrical supercapacitor. Even at 100 A g^{-1}, a high capacitance of 176 F g^{-1} was maintained.

3 Summary and Perspectives

PCMs are promising electrode materials for supercapacitors attributing to their rich precursors, low cost, high specific surface area, tunable pore structure, and good stability. PCMs could be prepared from various precursors including biomass, natural polymers, synthetic macromolecules, and carbon-rich small molecules by pyrolysis at high temperature. However, the carbonaceous products obtained from directly carbonization of precursors often show porous-less or even nonporous feature with limited SSA. It is necessary to improve the SSA and adjust the pore structure of carbon materials to enhance their capacitance performance. Physical/chemical activation methods are proved to be effective approaches.

Nowadays, PCMs have produced tons of kilograms annually through carbonization–activation way. However, there are some issues still unsolved which block the production and application of PCMs. As to the physical activation, steam and CO_2

are the commonly used activation agents which are low corrosive to the production facilities and more favorable for practical application. But physical activation always results in PCMs with narrowly distributed micropores, and the particle and microdomain sizes are reduced. Physical activation also shows the shortage in product yield, tap density, and SSA. As to chemical activation, corrosive reagents like $ZnCl_2$, KOH, NaOH, H_2SO_4, HNO_3, and K_2CO_3 are the traditional activation agents. Compared with physical activation, chemical activation shows advantages in relatively low activation temperature, high yield, large SSA, and high mesopore ratios. However, chemical activation often requires high mass ratio of corrosive activation agents to carbon sources and generates great amounts of contaminants. Hence, tradition chemical activation method is only limit to laboratory-scale research.

In recently years, great efforts have been investigated on the exploration of much less corrosive chemical activation agents and molten salts (KCl, NaCl, $CuCl_2$, $FeCl_3$, $NiCl_2$, etc.), decomposable salts (nitrates, carbonates, bicarbonates, acetates, oxalates, etc.), and oxidative salts ($KMnO_4$, $KClO_4$, $(NH_4)_2S_2O_8$, H_2O_2, etc.) are proved to be better choices. Among these new chemical activation agents, potassium salts and sodium salts are more preferred owing to their water solvable nature which are benefit for post-treatment. Moreover, potassium salts and sodium salts could be served as templates to generate hierarchical pores. Ammonium salts are also good choices attributing to their fully decomposable nature which could act as chemical blowing/foaming agents generating lots of macropores. Besides, ammonium salts could be used as nitrogen sources to introduce nitrogen species to contribute pseudocapacitance and modify the surface feature of carbon materials.

The pore structure optimization process is complicated and sometimes uncontrollable. It is very hard to obtain PCMs with idea pore structure from only one method within one-step experiments. As to application in supercapacitors, the ratio among macropores, mesopores, and micropores of PCMs should be well adjusted to keep a balance on specific capacitance, rate performance, stability, and tap density. From a production point of view, it is more favorable to synthesize PCMs from one-step carbonization and activation process with multifunctional agents (e.g., KCl, NaCl, NH_4NO_3). It is necessary to combine activation with other methods including template, chemical vapor deposition, electrospinning, hydrothermal/solvothermal method to design PCMs with finely tuned pore structures, and good capacitive performance.

References

Ahmed, S., Ahmed, A., Rafat, M.: Investigation on activated carbon derived from biomass Butnea monosperma and its application as a high performance supercapacitor electrode. J. Energy Storage **26** (2019). https://doi.org/10.1016/j.est.2019.100988

Bedia, J., Belver, C., Ponce, S., Rodriguez, J., Rodriguez, J.J.: Adsorption of antipyrine by activated carbons from $FeCl_3$-activation of Tara gum. Chem. Eng. J. **333**, 58–65 (2018). https://doi.org/10.1016/j.cej.2017.09.161

Bhat, V.S., Krishnan, S.G., Jayeoye, T.J., Rujiralai, T., Sirimahachai, U., Viswanatha, R., Khalid, M., Hegde, G.: Self-activated 'green' carbon nanoparticles for symmetric solid-state supercapacitors. J. Mater. Sci. (2021). https://doi.org/10.1007/s10853-021-06154-z

Bo, Y., Zhao, Y., Cai, Z., Bahi, A., Liu, C., Ko, F.: Facile synthesis of flexible electrode based on cotton/polypyrrole/multi-walled carbon nanotube composite for supercapacitors. Cellulose **25**(7), 4079–4091 (2018). https://doi.org/10.1007/s10570-018-1845-9

Borchardt, L., Zhu, Q.-L., Casco, M.E., Berger, R., Zhuang, X., Kaskel, S., Feng, X., Xu, Q.: Toward a molecular design of porous carbon materials. Mater. Today **20**(10), 592–610 (2017). https://doi.org/10.1016/j.mattod.2017.06.002

Budinova, T., Ekinci, E., Yardim, F., Grimm, A., Björnbom, E., Minkova, V., Goranova, M.: Characterization and application of activated carbon produced by H_3PO_4 and water vapor activation. Fuel Process. Technol. **87**(10), 899–905 (2006). https://doi.org/10.1016/j.fuproc.2006.06.005

Cai, R., Si, Y., You, B., Chen, M., Wu, L.: Yolk-shell carbon nanospheres with controlled structure and composition by self-activation and air activation. ACS Appl. Mater. Interfaces **12**(25), 28738–28749 (2020). https://doi.org/10.1021/acsami.0c02980

Cao, L., Li, H., Xu, Z., Gao, R., Wang, S., Zhang, G., Jiang, S., Xu, W., Hou, H.: Camellia pollen-derived carbon with controllable N content for high-performance supercapacitors by ammonium chloride activation and dual N-doping. ChemNanoMat **7**(1), 34–43 (2021). https://doi.org/10.1002/cnma.202000531

Chen, C., Yu, D., Zhao, G., Du, B., Tang, W., Sun, L., Sun, Y., Besenbacher, F., Yu, M.: Three-dimensional scaffolding framework of porous carbon nanosheets derived from plant wastes for high-performance supercapacitors. Nano Energy **27**, 377–389 (2016). https://doi.org/10.1016/j.nanoen.2016.07.020

Chen, W., Luo, M., Wang, X., Yang, K., Zhou, X.: Rapid synthesis of chitin-based porous carbons with high yield, high nitrogen retention, and low cost for high-rate supercapacitors. Int. J. Energy Res. **44**(2), 1167–1178 (2019). https://doi.org/10.1002/er.5008

Chen, W., Luo, M., Yang, K., Zhang, D., Zhou, X.: A clean and industrially applicable approach for the production of copper-doped and core-shell structured porous carbon microspheres as supercapacitor electrode materials. J. Cleaner Prod. **282** (2021). https://doi.org/10.1016/j.jclepro.2020.124534

Cheng, P., Gao, S., Zang, P., Yang, X., Bai, Y., Xu, H., Liu, Z., Lei, Z.: Hierarchically porous carbon by activation of shiitake mushroom for capacitive energy storage. Carbon **93**, 315–324 (2015). https://doi.org/10.1016/j.carbon.2015.05.056

Cheng, J., Hu, S.-C., Sun, G.-T., Kang, K., Zhu, M.-Q., Geng, Z.-C.: Comparison of activated carbons prepared by one-step and two-step chemical activation process based on cotton stalk for supercapacitors application. Energy **215** (2021). https://doi.org/10.1016/j.energy.2020.119144

Ding, Y., Li, Y., Dai, Y., Han, X., Xing, B., Zhu, L., Qiu, K., Wang, S.: A novel approach for preparing in-situ nitrogen doped carbon via pyrolysis of bean pulp for supercapacitors. Energy **216** (2021). https://doi.org/10.1016/j.energy.2020.119227

Elmouwahidi, A., Bailón-García, E., Pérez-Cadenas, A.F., Celzard, A., Fierro, V., Carrasco-Marín, F.: Carbon microspheres with tailored texture and surface chemistry as electrode materials for supercapacitors. ACS Sustain. Chem. Eng. **9**(1), 541–551 (2020). https://doi.org/10.1021/acssuschemeng.0c08024

Gao, Y., Tang, Y., Liu, W., Liu, L., Zeng, X.: Porous bamboo-like CNTs prepared by a simple and low-cost steam activation for supercapacitors. Int. J. Energy Res. **44**(13), 10946–10952 (2020a). https://doi.org/10.1002/er.5672

Gao, Y., Yue, Q., Gao, B., Li, A.: Insight into activated carbon from different kinds of chemical activating agents: a review. Sci. Total Environ. **746**, 141094 (2020b). https://doi.org/10.1016/j.scitotenv.2020.141094

Gao, Y., Sun, R., Li, A., Ji, G.: In-situ self-activation strategy toward highly porous biochar for supercapacitors: direct carbonization of marine algae. J. Electroanal. Chem. **882** (2021). https://doi.org/10.1016/j.jelechem.2021.114986

Gonzalez-Garcia, P.: Activated carbon from lingocellulosics precursors: a review of the synthesis methods, characterization techniques and applications. Renew. Sustain. Energy Rev. **82**, 1393–1414 (2018). https://doi.org/10.1016/j.rser.2017.04.117

Guo, N., Li, M., Wang, Y., Sun, X., Wang, F., Yang, R.: Soybean root-derived hierarchical porous carbon as electrode material for high-performance supercapacitors in ionic liquids. ACS Appl. Mater. Interfaces **8**(49), 33626–33634 (2016). https://doi.org/10.1021/acsami.6b11162

He, S., Chen, W.: 3D graphene nanomaterials for binder-free supercapacitors: scientific design for enhanced performance. Nanoscale **7**(16), 6957–6990 (2015). https://doi.org/10.1039/c4nr05895j

He, S., Chen, L., Xie, C., Hu, H., Chen, S., Hanif, M., Hou, H.: Supercapacitors based on 3D network of activated carbon nanowhiskers wrapped-on graphitized electrospun nanofibers. J. Power Sources **243**, 880–886 (2013). https://doi.org/10.1016/j.jpowsour.2013.06.104

He, J., Zhang, D., Han, M., Liu, X., Wang, Y., Li, Y., Zhang, X., Wang, K., Feng, H., Wang, Y.: One-step large-scale fabrication of nitrogen doped microporous carbon by self-activation of biomass for supercapacitors application. J. Energy Storage **21**, 94–104 (2019a). https://doi.org/10.1016/j.est.2018.11.015

He, S., Zhang, C., Du, C., Cheng, C., Chen, W.: High rate-performance supercapacitor based on nitrogen-doped hollow hexagonal carbon nanoprism arrays with ultrathin wall thickness in situ fabricated on carbon cloth. J. Power Sources **434**, 226701 (2019b). https://doi.org/10.1016/j.jpowsour.2019.226701

He, Y., Zhuang, X., Lei, C., Lei, L., Hou, Y., Mai, Y., Feng, X.: Porous carbon nanosheets: synthetic strategies and electrochemical energy related applications. Nano Today **24**, 103–119 (2019c). https://doi.org/10.1016/j.nantod.2018.12.004

Hou, L., Chen, Z., Zhao, Z., Sun, X., Zhang, J., Yuan, C.: Universal $FeCl_3$-activating strategy for green and scalable fabrication of sustainable biomass-derived hierarchical porous nitrogen-doped carbons for electrochemical supercapacitors. ACS Appl. Energy Mater. **2**(1), 548–557 (2018). https://doi.org/10.1021/acsaem.8b01589

Huang, C., Sun, T., Hulicova-Jurcakova, D.: Wide electrochemical window of supercapacitors from coffee bean-derived phosphorus-rich carbons. ChemSusChem **6**(12), 2330–2339 (2013). https://doi.org/10.1002/cssc.201300457

Huo, S., Zhang, X., Liang, B., Zhao, Y., Li, K.: Synthesis of interconnected hierarchically porous carbon networks with excellent diffusion ability based on $NaNO_3$ crystal-assisted strategy for high performance supercapacitors. J. Power Sources **450** (2020). https://doi.org/10.1016/j.jpowsour.2019.227612

Jin, Y., Tian, K., Wei, L., Zhang, X., Guo, X.: Hierarchical porous microspheres of activated carbon with a high surface area from spores for electrochemical double-layer capacitors. J. Mater. Chem. A **4**(41), 15968–15979 (2016). https://doi.org/10.1039/c6ta05872h

Kigozi, M., Kali, R., Bello, A., Padya, B., Kalu-Uka, G.M., Wasswa, J., Jain, P.K., Onwualu, P.A., Dzade, N.Y.: Modified activation process for supercapacitor electrode materials from African Maize Cob. Mater. **13**(23) (2020). https://doi.org/10.3390/ma13235412

Kim, C., Ngoc, B.T.N., Yang, K.S., Kojima, M., Kim, Y.A., Kim, Y.J., Endo, M., Yang, S.C.: Self-sustained thin webs consisting of porous carbon nanofibers for supercapacitors via the electrospinning of polyacrylonitrile solutions containing zinc chloride. Adv. Mater. **19**(17), 2341–2346 (2007). https://doi.org/10.1002/adma.200602184

Kim, M., Lim, H., Xu, X., Hossain, M.S.A., Na, J., Awaludin, N.N., Shah, J., Shrestha, L.K., Ariga, K., Nanjundan, A.K., Martin, D.J., Shapter, J.G., Yamauchi, Y.: Sorghum biomass-derived porous carbon electrodes for capacitive deionization and energy storage. Microporous Mesoporous Mater. **312** (2021). https://doi.org/10.1016/j.micromeso.2020.110757

Kumar, T.R., Senthil, R.A., Pan, Z., Pan, J., Sun, Y.: A tubular-like porous carbon derived from waste American poplar fruit as advanced electrode material for high-performance supercapacitor. J. Energy Storage **32** (2020). https://doi.org/10.1016/j.est.2020.101903

Lee, H.-M., Kwac, L.-K., An, K.-H., Park, S.-J., Kim, B.-J.: Electrochemical behavior of pitch-based activated carbon fibers for electrochemical capacitors. Energy Convers. Manage. **125**, 347–352 (2016). https://doi.org/10.1016/j.enconman.2016.06.006

Leng, C., Sun, K., Li, J., Jiang, J.: From dead pine needles to O, N codoped activated carbons by a one-step carbonization for high rate performance supercapacitors. ACS Sustain. Chem. Eng. **5**(11), 10474–10482 (2017). https://doi.org/10.1021/acssuschemeng.7b02481

Leng, C., Zhao, Z., Song, Y., Sun, L., Fan, Z., Yang, Y., Liu, X., Wang, X., Qiu, J.: 3D carbon frameworks for ultrafast charge/discharge rate supercapacitors with high energy-power density. Nano-Micro Lett. **13**(1) (2020). https://doi.org/10.1007/s40820-020-00535-w

Li, Y.-J., Ni, X.-Y., Shen, J., Liu, D., Liu, N.-P., Zhou, X.-W.: Preparation and performance of polypyrrole/nitric acid activated carbon aerogel nanocomposite materials for supercapacitors. Acta Phys. Chim. Sin. **32**(2), 493–502 (2016). https://doi.org/10.3866/pku.Whxb201511131

Li, Z.-Y., Akhtar, M.S., Kwak, D.-H., Yang, O.B.: Improvement in the surface properties of activated carbon via steam pretreatment for high performance supercapacitors. Appl. Surf. Sci. **404**, 88–93 (2017). https://doi.org/10.1016/j.apsusc.2017.01.238

Li, J., Wang, N., Tian, J., Qian, W., Chu, W.: Cross-coupled macro-mesoporous carbon network toward record high energy-power density supercapacitor at 4 V. Adv. Funct. Mater. **28**(51) (2018a). https://doi.org/10.1002/adfm.201806153

Li, Q., Wu, X., Zhao, Y., Miao, Z., Xing, L., Zhou, J., Zhao, J., Zhuo, S.: Nitrogen-doped hierarchical porous carbon through one-step activation of bean curd for high-performance supercapacitor electrode. ChemElectroChem **5**(12), 1606–1614 (2018b). https://doi.org/10.1002/celc.201800230

Li, Q., Mu, J., Zhou, J., Zhao, Y., Zhuo, S.: Avoiding the use of corrosive activator to produce nitrogen-doped hierarchical porous carbon materials for high-performance supercapacitor electrode. J. Electroanal. Chem. **832**, 284–292 (2019). https://doi.org/10.1016/j.jelechem.2018.11.013

Li, B., Xiong, H., Xiao, Y., Hu, J., Zhang, X., Li, L., Wang, R.: Efficient toluene adsorption on metal salt-activated porous carbons derived from low-cost biomass: a discussion of mechanism. ACS Omega **5**(22), 13196–13206 (2020a). https://doi.org/10.1021/acsomega.0c01230

Li, H., Cao, L., Wang, F., Duan, G., Xu, W., Mei, C., Zhang, G., Liu, K., Yang, M., Jiang, S.: *Fatsia japonica*-derived hierarchical porous carbon for supercapacitors with high energy density and long cycle life. Front. Chem. **8**, 89 (2020b). https://doi.org/10.3389/fchem.2020.00089

Li, Z., Guo, D., Liu, Y., Wang, H., Wang, L.: Recent advances and challenges in biomass-derived porous carbon nanomaterials for supercapacitors. Chem. Eng. J. **397** (2020c). https://doi.org/10.1016/j.cej.2020.125418

Li, P., Feng, C.-N., Li, H.-P., Zhang, X.-L., Zheng, X.-C.: Facile fabrication of carbon materials with hierarchical porous structure for high-performance supercapacitors. J. Alloys Compd. **851** (2021a). https://doi.org/10.1016/j.jallcom.2020.156922

Li, Y., Pu, Z., Sun, Q., Pan, N.: A review on novel activation strategy on carbonaceous materials with special morphology/texture for electrochemical storage. J. Energy Chem. **60**, 572–590 (2021b). https://doi.org/10.1016/j.jechem.2021.01.017

Liang, X., Liu, R., Wu, X.: Biomass waste derived functionalized hierarchical porous carbon with high gravimetric and volumetric capacitances for supercapacitors. Microporous Mesoporous Mater. **310** (2021). https://doi.org/10.1016/j.micromeso.2020.110659

Liu, T., Zhang, F., Song, Y., Li, Y.: Revitalizing carbon supercapacitor electrodes with hierarchical porous structures. J. Mater. Chem. A **5**(34), 17705–17733 (2017). https://doi.org/10.1039/c7ta05646j

Liu, S., Liang, Y., Zhou, W., Hu, W., Dong, H., Zheng, M., Hu, H., Lei, B., Xiao, Y., Liu, Y.: Large-scale synthesis of porous carbon via one-step $CuCl_2$ activation of rape pollen for high-performance supercapacitors. J. Mater. Chem. A **6**(25), 12046–12055 (2018). https://doi.org/10.1039/c8ta02838a

Lozano-Castelló, D., Calo, J.M., Cazorla-Amorós, D., Linares-Solano, A.: Carbon activation with KOH as explored by temperature programmed techniques, and the effects of hydrogen. Carbon **45**(13), 2529–2536 (2007). https://doi.org/10.1016/j.carbon.2007.08.021

Lv, Z., Li, X., Chen, X., Li, X., Wu, M., Li, Z.: One-step site-specific activation approach for preparation of hierarchical porous carbon materials with high electrochemical performance. ACS Appl. Energy Mater. **2**(12), 8767–8782 (2019). https://doi.org/10.1021/acsaem.9b01729

Ma, G., Yang, Q., Sun, K., Peng, H., Ran, F., Zhao, X., Lei, Z.: Nitrogen-doped porous carbon derived from biomass waste for high-performance supercapacitor. Biores. Technol. **197**, 137–142 (2015). https://doi.org/10.1016/j.biortech.2015.07.100

Ma, L., Liu, J., Lv, S., Zhou, Q., Shen, X., Mo, S., Tong, H.: Scalable one-step synthesis of N, S co-doped graphene-enhanced hierarchical porous carbon foam for high-performance solid-state supercapacitors. J. Mater. Chem. A **7**(13), 7591–7603 (2019). https://doi.org/10.1039/c9ta00038k

Mao, Y., Xie, H., Chen, X., Zhao, Y., Qu, J., Song, Q., Ning, Z., Xing, P., Yin, H.: A combined leaching and electrochemical activation approach to converting coal to capacitive carbon in molten carbonates. J. Cleaner Prod. **248** (2020). https://doi.org/10.1016/j.jclepro.2019.119218

Merlet, C., Rotenberg, B., Madden, P.A., Taberna, P.L., Simon, P., Gogotsi, Y., Salanne, M.: On the molecular origin of supercapacitance in nanoporous carbon electrodes. Nat. Mater. **11**(4), 306–310 (2012). https://doi.org/10.1038/nmat3260

Mo, C., Zhang, J., Zhang, G.: Hierarchical porous carbon with three dimensional nanonetwork from water hyacinth leaves for energy storage. J. Energy Storage **32** (2020). https://doi.org/10.1016/j.est.2020.101848

Mohamedkhair, A.K., Aziz, M.A., Shah, S.S., Shaikh, M.N., Jamil, A.K., Qasem, M.A.A., Buliyaminu, I.A., Yamani, Z.H.: Effect of an activating agent on the physicochemical properties and supercapacitor performance of naturally nitrogen-enriched carbon derived from *Albizia procera* leaves. Arab. J. Chem. **13**(7), 6161–6173 (2020). https://doi.org/10.1016/j.arabjc.2020.05.017

Myglovets, M., Poddubnaya, O.I., Sevastyanova, O., Lindström, M.E., Gawdzik, B., Sobiesiak, M., Tsyba, M.M., Sapsay, V.I., Klymchuk, D.O., Puziy, A.M.: Preparation of carbon adsorbents from lignosulfonate by phosphoric acid activation for the adsorption of metal ions. Carbon **80**, 771–783 (2014). https://doi.org/10.1016/j.carbon.2014.09.032

Navarro, R.M., Peña, M.A., Fierro, J.L.G.: Hydrogen production reactions from carbon feedstocks: fossil fuels and biomass. Chem. Rev. **107**(10), 3952–3991 (2007). https://doi.org/10.1021/cr0501994

Nishihara, H., Kyotani, T.: Templated nanocarbons for energy storage. Adv. Mater. **24**(33), 4473–4498 (2012). https://doi.org/10.1002/adma.201201715

Niu, J., Shao, R., Liang, J., Dou, M., Li, Z., Huang, Y., Wang, F.: Biomass-derived mesopore-dominant porous carbons with large specific surface area and high defect density as high performance electrode materials for Li-ion batteries and supercapacitors. Nano Energy **36**, 322–330 (2017). https://doi.org/10.1016/j.nanoen.2017.04.042

Olivares-Marín, M., Fernández-González, C., Macías-García, A., Gómez-Serrano, V.: Thermal behaviour of lignocellulosic material in the presence of phosphoric acid. Influence of the acid content in the initial solution. Carbon **44**(11), 2347–2350 (2006). https://doi.org/10.1016/j.carbon.2006.04.004

Pallarés, J., González-Cencerrado, A., Arauzo, I.: Production and characterization of activated carbon from barley straw by physical activation with carbon dioxide and steam. Biomass Bioenerg. **115**, 64–73 (2018). https://doi.org/10.1016/j.biombioe.2018.04.015

Pourhosseini, S.E.M., Norouzi, O., Naderi, H.R.: Study of micro/macro ordered porous carbon with olive-shaped structure derived from *Cladophora glomerata* macroalgae as efficient working electrodes of supercapacitors. Biomass Bioenerg. **107**, 287–298 (2017). https://doi.org/10.1016/j.biombioe.2017.10.025

Qin, L.: Porous carbon derived from pine nut shell prepared by steam activation for supercapacitor electrode material. Int. J. Electrochem. Sci. 8907–8918 (2019). https://doi.org/10.20964/2019.09.20

Qiu, D., Guo, N., Gao, A., Zheng, L., Xu, W., Li, M., Wang, F., Yang, R.: Preparation of oxygen-enriched hierarchically porous carbon by $KMnO_4$ one-pot oxidation and activation: mechanism

and capacitive energy storage. Electrochim. Acta **294**, 398–405 (2019a). https://doi.org/10.1016/j.electacta.2018.10.049

Qiu, D., Kang, C., Gao, A., Xie, Z., Li, Y., Li, M., Wang, F., Yang, R.: Sustainable low-temperature activation to customize pore structure and heteroatoms of biomass-derived carbon enabling unprecedented durable supercapacitors. ACS Sustain. Chem. Eng. **7**(17), 14629–14638 (2019b). https://doi.org/10.1021/acssuschemeng.9b02425

Qiu, S., Chen, Z., Zhuo, H., Hu, Y., Liu, Q., Peng, X., Zhong, L.: Using $FeCl_3$ as a solvent, template, and activator to prepare B, N Co-doping porous carbon with excellent supercapacitance. ACS Sustain. Chem. Eng. **7**(19), 15983–15994 (2019c). https://doi.org/10.1021/acssuschemeng.9b02431

Sevilla, M., Fuertes, A.B.: A green approach to high-performance supercapacitor electrodes: the chemical activation of hydrochar with potassium bicarbonate. ChemSusChem **9**(14), 1880–1888 (2016). https://doi.org/10.1002/cssc.201600426

Sevilla, M., Diez, N., Fuertes, A.B.: More sustainable chemical activation strategies for the production of porous carbons. ChemSusChem **14**(1), 94–117 (2021). https://doi.org/10.1002/cssc.202001838

Shi, Y., Liu, G., Wang, L., Zhang, H.: Heteroatom-doped porous carbons from sucrose and phytic acid for adsorptive desulfurization and sulfamethoxazole removal: a comparison between aqueous and non-aqueous adsorption. J. Colloid Interface Sci. **557**, 336–348 (2019). https://doi.org/10.1016/j.jcis.2019.09.032

Simon, P., Gogotsi, Y., Dunn, B.: Where do batteries end and supercapacitors begin? Science **343**(6176), 1210–1211 (2014). https://doi.org/10.1126/science.1249625

Son, Y.-R., Park, S.-J.: Preparation and characterization of mesoporous activated carbons from nonporous hard carbon via enhanced steam activation strategy. Mater. Chem. Phys. **242** (2020). https://doi.org/10.1016/j.matchemphys.2019.122454

Sun, F., Wu, D., Gao, J., Pei, T., Chen, Y., Wang, K., Yang, H., Zhao, G.: Graphitic porous carbon with multiple structural merits for high-performance organic supercapacitor. J. Power Sources **477** (2020). https://doi.org/10.1016/j.jpowsour.2020.228759

Tang, D., Luo, Y., Lei, W., Xiang, Q., Ren, W., Song, W., Chen, K., Sun, J.: Hierarchical porous carbon materials derived from waste *Lentinus edodes* by a hybrid hydrothermal and molten salt process for supercapacitor applications. Appl. Surf. Sci. **462**, 862–871 (2018). https://doi.org/10.1016/j.apsusc.2018.08.153

Thileep Kumar, K., Sivagaami Sundari, G., Senthil Kumar, E., Ashwini, A., Ramya, M., Varsha, P., Kalaivani, R., Shanmugaraj Andikkadu, M., Kumaran, V., Gnanamuthu, R., Karazhanov, S.Z., Raghu, S.: Synthesis of nanoporous carbon with new activating agent for high-performance supercapacitor. Mater. Lett. **218**, 181–184 (2018). https://doi.org/10.1016/j.matlet.2018.02.017

Tian, Y., Xiao, C., Yin, J., Zhang, W., Bao, J., Lin, H., Lu, H.: Hierarchical porous carbon prepared through sustainable $CuCl_2$ activation of rice husk for high-performance supercapacitors. ChemistrySelect **4**(8), 2314–2319 (2019). https://doi.org/10.1002/slct.201804002

Tian, W., Zhang, H., Duan, X., Sun, H., Shao, G., Wang, S.: Porous carbons: structure-oriented design and versatile applications. Adv. Func. Mater. **30**(17), 1909265 (2020). https://doi.org/10.1002/adfm.201909265

Veerakumar, P., Maiyalagan, T., Raj, B.G.S., Guruprasad, K., Jiang, Z., Lin, K.-C.: Paper flower-derived porous carbons with high-capacitance by chemical and physical activation for sustainable applications. Arab. J. Chem. **13**(1), 2995–3007 (2020). https://doi.org/10.1016/j.arabjc.2018.08.009

Vinayagam, M., Suresh Babu, R., Sivasamy, A., Ferreira de Barros, A.L.: Biomass-derived porous activated carbon from *Syzygium cumini* fruit shells and *Chrysopogon zizanioides* roots for high-energy density symmetric supercapacitors. Biomass Bioenergy **143** (2020). https://doi.org/10.1016/j.biombioe.2020.105838

Wang, J., Kaskel, S.: KOH activation of carbon-based materials for energy storage. J. Mater. Chem. **22**(45), 23710 (2012). https://doi.org/10.1039/c2jm34066f

Wang, Y., Song, Y., Xia, Y.: Electrochemical capacitors: mechanism, materials, systems, characterization and applications. Chem. Soc. Rev. **45**(21), 5925–5950 (2016). https://doi.org/10.1039/c5cs00580a

Wang, D., Liu, S., Jiao, L., Fang, G., Geng, G., Ma, J.: Unconventional mesopore carbon nanomesh prepared through explosion–assisted activation approach: a robust electrode material for ultrafast organic electrolyte supercapacitors. Carbon **119**, 30–39 (2017). https://doi.org/10.1016/j.carbon.2017.03.102

Wang, C., Wu, D., Wang, H., Gao, Z., Xu, F., Jiang, K.: A green and scalable route to yield porous carbon sheets from biomass for supercapacitors with high capacity. J. Mater. Chem. A **6**(3), 1244–1254 (2018). https://doi.org/10.1039/c7ta07579k

Wang, Y., Qu, Q., Gao, S., Tang, G., Liu, K., He, S., Huang, C.: Biomass derived carbon as binder-free electrode materials for supercapacitors. Carbon **155**, 706–726 (2019). https://doi.org/10.1016/j.carbon.2019.09.018

Wang, F., Chen, L., Li, H., Duan, G., He, S., Zhang, L., Zhang, G., Zhou, Z., Jiang, S.: N-doped honeycomb-like porous carbon towards high-performance supercapacitor. Chin. Chem. Lett. **31**(7), 1986–1990 (2020a). https://doi.org/10.1016/j.cclet.2020.02.020

Wang, H., Shao, Y., Mei, S., Lu, Y., Zhang, M., Sun, J.K., Matyjaszewski, K., Antonietti, M., Yuan, J.: Polymer-derived heteroatom-doped porous carbon materials. Chem. Rev. **120**(17), 9363–9419 (2020b). https://doi.org/10.1021/acs.chemrev.0c00080

Wang, Y., Zhang, L., Hou, H., Xu, W., Duan, G., He, S., Liu, K., Jiang, S.: Recent progress in carbon-based materials for supercapacitor electrodes: a review. J. Mater. Sci. **56**(1), 173–200 (2020c). https://doi.org/10.1007/s10853-020-05157-6

Wang, A., Sun, K., Xu, R., Sun, Y., Jiang, J.: Cleanly synthesizing rotten potato-based activated carbon for supercapacitor by self-catalytic activation. J. Cleaner Prod. **283** (2021). https://doi.org/10.1016/j.jclepro.2020.125385

Yakaboylu, G.A., Jiang, C., Yumak, T., Zondlo, J.W., Wang, J., Sabolsky, E.M.: Engineered hierarchical porous carbons for supercapacitor applications through chemical pretreatment and activation of biomass precursors. Renew. Energy **163**, 276–287 (2021). https://doi.org/10.1016/j.renene.2020.08.092

Yan, B., Zheng, J., Wang, F., Zhao, L., Zhang, Q., Xu, W., He, S.: Review on porous carbon materials engineered by ZnO templates: design, synthesis and capacitance performance. Mater. Design **201**, 109518 (2021)

Yi, S., Qin, X., Liang, C., Li, J., Rajagopalan, R., Zhang, Z., Song, J., Tang, Y., Cheng, F., Wang, H., Shao, M.: Insights into $KMnO_4$ etched N-rich carbon nanotubes as advanced electrocatalysts for Zn-air batteries. Appl. Catal. B Environ. **264** (2020). https://doi.org/10.1016/j.apcatb.2019.118537

Yin, J., Zhang, W., Alhebshi, N.A., Salah, N., Alshareef, H.N.: Synthesis strategies of porous carbon for supercapacitor applications. Small Methods **4**(3) (2020). https://doi.org/10.1002/smtd.201900853

Yu, D., Ma, Y., Chen, M., Dong, X.: KOH activation of wax gourd-derived carbon materials with high porosity and heteroatom content for aqueous or all-solid-state supercapacitors. J. Colloid Interface Sci. **537**, 569–578 (2019). https://doi.org/10.1016/j.jcis.2018.11.070

Zeng, F., Kuang, Y., Zhang, N., Huang, Z., Pan, Y., Hou, Z., Zhou, H., Yan, C., Schmidt, O.G.: Multilayer super-short carbon nanotube/reduced graphene oxide architecture for enhanced supercapacitor properties. J. Power Sources **247**, 396–401 (2014). https://doi.org/10.1016/j.jpowsour.2013.08.122

Zhai, Y., Dou, Y., Zhao, D., Fulvio, P.F., Mayes, R.T., Dai, S.: Carbon materials for chemical capacitive energy storage. Adv. Mater. **23**(42), 4828–4850 (2011). https://doi.org/10.1002/adma.201100984

Zhang, Z., Lei, Y., Li, D., Zhao, J., Wang, Y., Zhou, G., Yan, C., He, Q.: Sudden heating of H_3PO_4-loaded coconut shell in CO_2 flow to produce super activated carbon and its application for benzene adsorption. Renew. Energy **153**, 1091–1099 (2020). https://doi.org/10.1016/j.renene.2020.02.059

Zhu, Z., Xu, Z.: The rational design of biomass-derived carbon materials towards next-generation energy storage: a review. Renew. Sustain. Energy Rev. **134** (2020). https://doi.org/10.1016/j.rser.2020.110308

Zhu, K., Wang, Y., Tang, J.A., Guo, S., Gao, Z., Wei, Y., Chen, G., Gao, Y.: A high-performance supercapacitor based on activated carbon fibers with an optimized pore structure and oxygen-containing functional groups. Mater. Chem. Front. **1**(5), 958–966 (2017). https://doi.org/10.1039/c6qm00196c

Zhu, S., Zhao, N., Li, J., Deng, X., Sha, J., He, C.: Hard-template synthesis of three-dimensional interconnected carbon networks: rational design, hybridization and energy-related applications. Nano Today **29**, 100796 (2019). https://doi.org/10.1016/j.nantod.2019.100796

Zong, S., Zhang, Y., Xaba, M.S., Liu, X., Chen, A.: N-doped porous carbon nanotubes derived from polypyrrole for supercapacitors with high performance. J. Anal. Appl. Pyrol **152** (2020). https://doi.org/10.1016/j.jaap.2020.104925